2021 43rd Annual International Conference of the
IEEE Engineering in Medicine & Biology Society (EMBC)
Oct 31 - Nov 4, 2021. Virtual Conference

Lower limb prosthesis: Optimization by lattice and four-bar polycentric knee

Enrique Contreras-Tenorio [1], Ilse Kardasch-Nava [1], Shazer González de Salceda [1],
Rubén Fuentes-Alvarez [1,2,*], *Member, IEEE*, Juan Alfonso Beltrán Fernández [3],
Karla Rincón-Martínez [1], Mariel Alfaro-Ponce [1], *Member, IEEE* and Iván Matehuala-Morán [1,2]

***Abstract*—Diabetes has brought several health problems; one of the most common is the amputation of the lower limb, for which the development of low-cost lower limb prostheses has taken on an important role to allow people with these injuries to continue independently with their lives. This paper proposes developing a transfemoral prosthesis for a 47-year-old patient with a weight of 100kg and a height of 1.80m. The approach shows the kinematic model of the four-bar mechanism of the knee, following the Denavith-Hartenberg method, and the calculation of the knee angle curve and the gait with the help of *OpenSim*. Consequently, it is shown the design of the parts of the prosthesis done in *Autodesk Fusion 360* and their optimization by a lattice in *Creo* software. Finally, the stress simulations in *Ansys* with the materials previously selected in *CES EduPack* are presented.**

***Index Terms*—Knee biomechanics, Lattice optimization, Lower-limb prosthesis.**

I. INTRODUCTION

Between 2004 and 2013, the Mexican Social Security Institute (IMSS) concluded that the index of major amputations due to *Diabetes Mellitus* (DM) was 100.9 per 100,000 subjects in 2004 and 111.1 per 100,000 subjects in 2013 [1]. In 2017 it was estimated that 57.7 million people were living with limb amputation due to traumatic causes, including amputations related to DM [1]. Based on these prevalence estimates, approximately 75,850 prostheses are needed globally to treat people with traumatic amputations [2]. Therefore, to improve the patient quality of life and to help them increase their independence, it is essential to place a prosthesis [3]. This prosthesis must be manufactured considering several factors such as friction, adhesion, stiffness, length design and deformation that the material can withstand, so patients may have better control of the prosthesis with as little pain and as much comfort as possible [4]. Finally, the most important factor to consider is the type of prosthesis that the patient needs. For the lower limb, a prosthesis is made according to the patient's type of amputation and characteristics, i.e. height, weight, and activity level. For transfemoral amputations, some prostheses are knee disarticulation prosthesis, femoral prosthesis, hip disarticulation and above-knee prosthesis. For prosthetic knees, the type of prosthesis depends on the joint, which acts as an element that absorbs energy from the impacts received when walking or running [5]. Although the knees have 6 degrees of freedom (DOF), the flexion-extension movement in the sagittal plane in two dimensions is the most important due to its polycentric character, which allows maintaining the Instantaneous Center of Rotation (ICR) of the body aligned to the Trochanter-Knee-Ankle (TKA) line. However, they can still be classified into two major groups depending on their number of axes: monocentric (single axis of rotation) and polycentric (can alter their axis of rotation and have better control of the knee to give a more natural and closer movement to the body's biomechanics).

The design of polycentric knees is generally composed of a 4-bar mechanisms, where the position of the center of rotation is altered according to the individual's position. These prostheses' ability to better mimic natural movements is more comfortable for patients and gives excellent stability and ease during walking. Additionally, unlike monocentric knees, they can improve the swing phase of a normal walk [6] and allow the patient to have different kinds of motion such as: oscillation, rotation, or a combination of both [6]. Also, they are suitable for patients that have a short residual limb; they are more aesthetic; and, during flexion, the toe has greater slack because of the relative dorsiflexion of the foot [7]. The main negative features are their cost, the large amount of maintenance they require and their shorter lifespan.

Finally, in recent studies about transfemoral prosthesis' design, such as: [8], it is described the static analysis and kinematic and kinetic study of the four-bar mechanism, where it is considered the generation of the trajectory of the ICR. However, the prosthesis should not exceed a load of 100 kg, and it must have cushioning to help dissipate the energy of the knee during walking.

*This work was supported by Tecnológico de Monterrey.

[1]E. Contreras-Tenorio, I. Kardasch-Nava, S. González de Salceda, R. Fuentes-Alvarez*, K. Rincón-Martínez, M. Alfaro-Ponce and I. Matehuala-Morán are with Tecnológico de Monterrey, School of Engineering and Sciences, Calle del Puente 222, Col. Ejidos de Huipulco Tlalpan, 14380, CDMX, Mexico.

[2]R. Fuentes-Alvarez* and I. Matehuala-Morán are with Instituto Nacional de Ciencias Médicas y Nutrición Salvador Zubirán, Biomedical Engineering Department, Tlalpan, CDMX, 14080, Mexico. *joru.fua@gmail.com

[3]J. A. Beltrán Fernández is with Instituto Politécnico Nacional, Escuela Superior de Ingeniería Mecánica y Eléctrica, SEPI-Zacatenco, Gustavo A. Madero, CDMX, 14080, Mexico.

A. Paper Structure

In this paper, Section II describes the problems related to the design of the lower limb. Section III introduces the kinematic model of the four-bar polycentric knee. Section IV presents the description of the material selection, the structural design of the lower limb and the static analysis simulations made in *Ansys Workbench*. Section V shows the results of the prosthesis design, which are discussed in section VI. Lastly, section VII comments in more detail the conclusions of this work.

II. Problem Statement

Over the years, the design of lower limb prostheses has evolved, where a crucial factor has been considering the material used for each part of the transfemoral prosthesis (foot, pylon, knee and knee socket). If careful analyses of the materials and design are not made, the patient's health can be compromised. On the one hand, mechanical injuries can cause blisters, oedema, callosities, cellulitis, hyperkeratosis, etc. On the other hand, sweating can cause miliaria, hidradenitis, skin rash and irritation. Additionally, a lousy adjustment can lead to folliculitis, pyoderma or acroangiodermatitis.

Moreover, if bacterias or fungi are present, the patient may present irritation, folliculitis, cellulitis, or other symptoms [9]. In this work, a transfemoral prosthesis is designed for a 47-year-old person with an amputation due to DM. With the following characteristics: a weight of 100kg and a height of 1.80m. The work is focused on the knee, pylon and foot. Regarding the design of the knee, it consists of a four-bar mechanism whose kinematic model is obtained throughout the Denavit-Hartenberg (DH) theory (which theoretical ground can be consulted in [10]) and whose configuration reduces the friction between the moving parts due to its polycentric character [11]. In addition, the lattice configuration of the foot and the material selection of this part give the mechanism a damping system and reduce the amount of material needed to build the prosthesis. Therefore, the patient already possesses a socket that can be adjusted to this design of the transfemoral prosthesis. The socket analysis will be done in future work.

III. Kinematic Modeling

For the mathematical model of the leg, it was necessary to use a tomography to scale and obtain the patient's model. This helps determine the reference point, place markers in points of interest with the software *OpenSim* [12], [13] and verify if there is a correct trajectory of the lower limb prosthesis during the gait cycle [14]–[17]. To perform the kinematics of the lower limb, it is established that the leg is a complex mechanical system since it has 21 DOF. However, it is possible to accurately model the movements of the leg by simplifying a 9 DOF mechanism; this is shown in Figure 1. Nonetheless, some of the assumptions that need to be made for this 9 DOF model are: the leg is modelled as a serial robot; the hip joint is modelled as a perfect ball joint; standard DH configuration is used and the ankle joint complex is locked for robotic manipulation, and it is rigid [18].

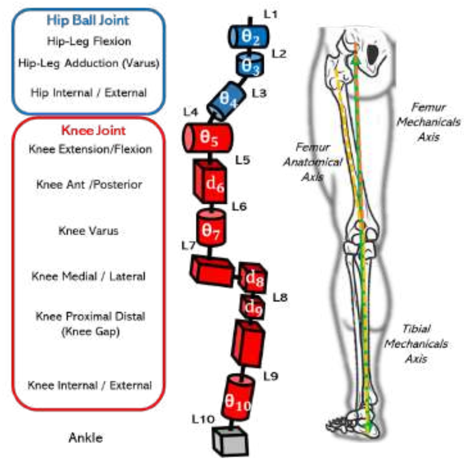

Figure 1. TKA line and the kinematic model of the leg (9 DOF) using DH [18].

In this section, the analysis of the kinematic model of the polycentric knee is presented, assuming that the mechanism is an open kinematic chain composed of two rigid bodies connected to a four-bar mechanism that has 6 DOF (Figure 2).

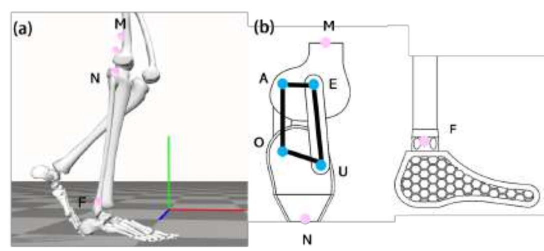

Figure 2. Convention of the four-bar mechanism. a) Shows *OpenSim*'s markers as a pink dot regrading roll-pitch-yaw coordinates points:M at $[0.0150174, -0.36972, 0.0928795]$, N at $[-0.004347, -0.459433, 0.0912315]$, and F at $[0.01, -0.38, 0.1]$. b) Markers of each link of the proposed mechanism.

The positions of each of the points E, U, N and F, relative to the fixed coordinate frame at point M, are known by using the DH convention. In which a transformation T_i^j is established by changing any point from the reference frame $i_{(x,y,z)}$ to the reference frame $j_{(x,y,z)}$. The transformations for the four-bar knee are presented in the system of equations 1.

$$T_E^M = \begin{bmatrix} \cos\phi & \sin\phi & |E|\cos\phi \\ -\sin\phi & \cos\phi & |E|\sin\phi \\ 0 & 0 & 1 \end{bmatrix}, T_U^E = \begin{bmatrix} \cos\gamma & -\sin\gamma & |EU|\cos\gamma \\ \sin\gamma & \cos\gamma & |EU|\sin\gamma \\ 0 & 0 & 1 \end{bmatrix}, \quad (1)$$

$$T_N^U = \begin{bmatrix} \cos\delta & -\sin\delta & |UN|\cos\delta \\ \sin\delta & \cos\delta & |UN|\sin\delta \\ 0 & 0 & 1 \end{bmatrix}, T_F^N = \begin{bmatrix} \cos\delta_2 & -\sin\delta_2 & |NF|\cos\delta_2 \\ \cos\delta_2 & \cos\delta_2 & |NF|\sin\delta_2 \\ 0 & 0 & 1 \end{bmatrix}$$

Where the angle ϕ_i of a transformation T_i^j is defined as the angle between the x_j-axis and x_i-axis. For instance in T_U^E, γ is the angle from x_E-axis to x_U-axis.

And to know the coordinates of the points of interest N and F, the following transformations concerning the desired reference frame $M_{(x,y,z)}$ need to be made.

$$T_N^M = T_E^M T_U^E T_N^U, \quad T_F^M = T_E^M T_U^E T_N^U T_F^N \tag{2}$$

Since these transformations depend on the angles ϕ, γ, δ and δ_2 and, therefore, on the coordinates of points A, E, O and U, it is necessary to obtain the coordinates of points A and O by using the equations for a four-bar mechanism (Eq. 3), proposed by Robert L. Norton [19]. It is important to clarify that these equations are for the reference frame $E_{(x,y,z)}$, so at the end, the transformation T_E^M must be used to obtain the coordinates in the frame $M_{(x,y,z)}$.

$$O_y = \frac{-Q \pm \sqrt{Q^2 - 4PR}}{2P}, \quad O_x = -S - \frac{U_y O_y}{U_x - |AE|} \tag{3}$$

Where P, Q, R and S are given by:

$$P = \frac{U_y^2}{(U_x - |AE|)^2} + 1, \quad R = -(|AE| - S)^2 - |AO|^2 \tag{4}$$

$$Q = \frac{2U_y(|AE| - S)}{U_x - |AE|}, \quad S = \frac{|EU|^2 - |OU|^2 + |AO|^2 - |AE|^2}{2(U_x - |AO|)}$$

A. Optimization

The error of the trajectory that the coordinates of the points E, U, O and A of the prosthesis was minimized by making an iterative process in *Matlab*. This process compares the error of the prosthetic model concerning the trajectory of the *OpenSim*'s model. In order to calculate the error, an interpolation between the point N with coordinates (x, y) was done in order to obtain the trajectories $y(x)$ with respect to the reference $y_{Ref}(x)$.

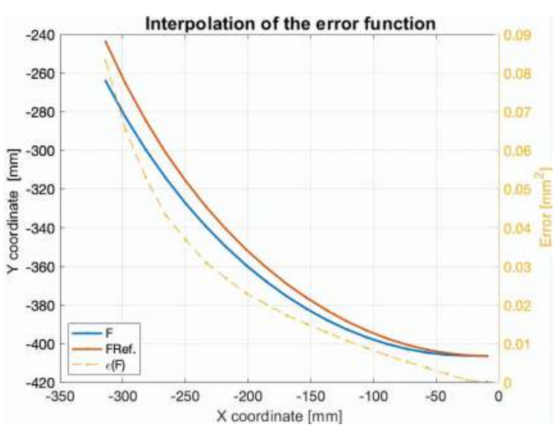

Figure 3. Trajectory interpolation of point F (blue), in which the error is emphasized to show what happens when the trajectory is not optimized.

The same process was repeated with point F and the total error was the sum of both errors, i.e, $\epsilon_T = \epsilon_N + \epsilon_F$. The equation of the error between curves (the trajectory of point N or F) is defined by:

$$\epsilon = \sum (y - y_{ref})^2 \tag{5}$$

The algorithm was optimized, so the error function was smaller than $1e^{-10}$. In order to do so, the coordinates A, E, O, and U were modified until this happened. The trajectories and error are shown in Figure 3.

B. Evaluation

The average relative errors of the trajectories of the coordinates A, E, U and O was obtained with the equation below. With this procedure, it was possible to determine the maximum error and look for outlier values.

$$Err = \frac{1}{n} \sum_{i=1}^{n} \frac{y - y_{ref}}{y_{ref}} \tag{6}$$

Also, a trajectory test was done with the Computer-Aided Design (CAD), and different values of γ were given to obtain the absolute error between the analytical trajectory and the trajectory made by the prosthesis.

C. Shock absorb design

After selecting the prosthesis material, the CAD files were joined using revolute joints, and a dynamic simulation was performed with *SimScape Multibody*. An array of the values of the angle $\gamma(t)$, which is the angle between bars EA and EU, was done to obtain the tibia's position and angular velocity data. In this equation, ϕ_k corresponds to the knee angle during walking, ω_k to the angular velocity of the tibia, k to the elastic constant, and δ_k to the damping coefficient. And with Eq. 7, the moment of the knee during the gait cycle was known.

$$M = k\phi_k + \delta_k \omega_k \tag{7}$$

With the reference data of the knee moment, obtained from [20], an optimization of the variables k and δ_k was performed. The moments of the prosthesis were adjusted so they would emulate those exerted during the natural gait cycle. In the trajectory optimization, the data was interpolated, and the error function was obtained.

IV. Materials and Methods

A lower limb prosthesis can be divided as seen in Figure 4 and should be composed of materials that have high tensile strength to reduce the slippage and pistoning that occurs in the gait cycle. However, it should also be considered the friction, adhesion, stiffness and deformation that the materials can withstand. To select the materials for the prosthesis, the *CES EduPack* software was used. According to the mechanical, physical or chemical properties needed to suit specific application requirements, this software filters the materials. For the socket, the comparison was made between plastics [21], but for the pylon, knee and foot, the comparison was based on metallic materials [22] and carbon fiber [23].

Table I
PROPERTIES OF THE MATERIALS FOR THE TRANSFEMORAL PROSTHESIS

Material *	Compressive strength [MPa]*	Tensile strength [MPa]*	Density [kg/m3]*	Poisson's ratio*	Elongation [%]*	Young's modulus [GPa]*
Polyethylene	19.7-31.9	20.7-44.8	939-960	0.41-0.43	200-800	0.62-0.90
Carbon Fiber, high strength	4900-5000	4400-4800	1800-1840	0.01-0.2	1.7-2	225-260
Aluminum 7068	655-764	648-756	2850	0.33-0.343	5-7.2	71.2-74.8

* Mechanical properties taken from the software *CES EduPack*.

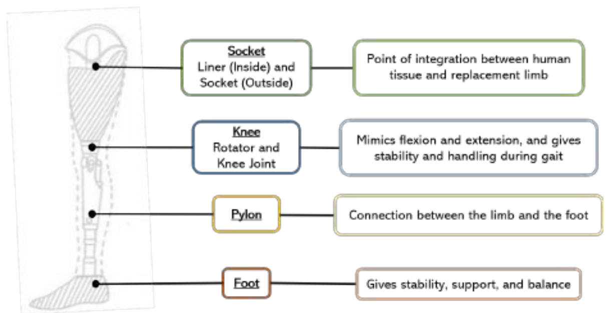

Figure 4. The design of a transfemoral prosthesis can be divided in four blocks: socket, knee, pylon and foot.

Since the socket will be subjected to stress, it was decided to analyze the compressive strength and the elongation to know if the material can withstand compressive forces without breaking and return to its initial position without suffering deformations. Materials with a greater interval of elongation are polyethene and polypropylene. Furthermore, these materials can withstand compressive strengths of about 25MPa, which means that the socket can bear the load of the patient's weight and it does not break. Thus, with the information gathered, it can be seen that polyethene is a good option for the socket since it has a lower density, withstands the forces caused by the limb, avoids problems related to sweating, and the price per kilogram is accessible. It is also more flexible than polypropylene and allows to mold sockets with ease [21]. In the case of the pylon, knee and foot, a similar analysis was made. Nonetheless, it was considered that the knee and pylon would be composed of a rigid material, whilst the foot needed to be made out of a more flexible material that could act as a damper. Considering that the safety factor of the prosthesis should be at least two or greater, that the density of the material should be light and that it must withstand the weight of the patient, it was seen that the aluminum 7068 (Al-7068) and carbon fibre could provide these design specifications. Making the Al-7068 a good option for the pylon and knee and the carbon fibre a good choice for the foot. Also, carbon fibres withstand more compressive strengths than some metals and plastics. Also, they have an elongation higher than 0.1% and lower than 10%. Simultaneously, aluminum can withstand compressive strengths greater than 100 MPa and have a greater elongation than carbon fibres but lower than plastics. Finally, Table 1 shows the most relevant mechanical and physical properties of the materials used for the transfemoral prosthesis.

A. Structural Design

It is crucial to remember that a limb amputation design can generate unpleasant psychological consequences, as multiple investigations have shown. This is mainly in the later phase of the amputation, where stress and depression and the null possibility of accepting a new anatomical condition. So beyond the functionality of the prosthesis, it is imperative the aesthetic quality of it, which has a significant weight in the psychology of amputee patients as described in the theory of the Uncanny Valley, which attempts to describe the level of familiarity and human likeness of various entities through the level of acceptance that observers show towards them [24]. Moreover, it is essential to keep in mind the load line for the stability of the prosthesis (Figure 5). Thus, the location and direction of the load line can be measured by a force plate during gait, and it is constantly changing its location and direction concerning the long geometric axis of the prosthesis [25]. The pylon and knee design feature casings provide an aesthetic appearance and protection to the rest of the interior parts; these are designed based on the contour of the leg's front and side views. Afterwards, the foot model proposed has a light structure, adaptability to different walking speeds, safety when walking, the necessary support when standing, and considerable helpful life.

B. Lattice Optimization

A lattice with a hexagonal cell shape on a closed body, cell size 25 x 25, with a wall thickness of 2mm and rounding radius 0.8mm, was realized in *Creo* software.

The lattice optimization changes the geometry of the foot and allows a reduction of material greater than 70% of the initial weight. The weight before this reduction was 1.779kg, whereas after it was 0.530kg. Besides, since carbon fibre was used for the foot, this part of the body became flexible and helped dissipate and withstand

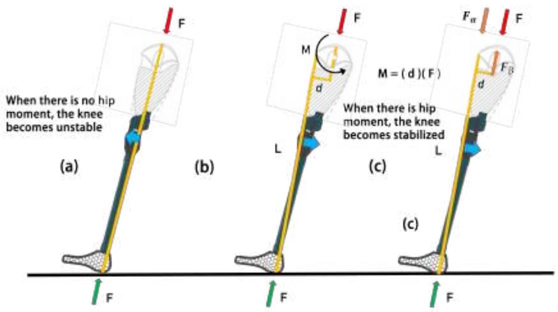

Figure 5. Free body diagram of the proposed prosthesis. a) The load line (yellow line) is passing behind the knee when the heel touches the ground. This line goes from the ankle to the joint located in the hip and its direction is related to the knee's stability (blue arrows). F represents the normal force that is produced when the ground pushes back on the heel; its magnitude is the same as the force acting on the socket, but in the opposite direction. Since the force is acting directly on the load line, this produces the knee to buckle when the load of the weight acts upon the mechanism. b) The combination of the joint force and extension moment acting on the hip joint produces a stabilization of the knee. M represents the extension moment, and d is the distance between the force exerted on the socket and the normal force. c) The moment in (b) can be replaced with forces F_α and F_β separated by a distance d. By doing this, F and F_β cancel each other out.

the stresses, thus reducing the damage to the stump. The type of scaffold structure was proposed to decrease the rigidity of the support system. However, the term damping was not associated with viscoelasticity, but rather with energy dissipation through reduction of mass by matrix arrangement using scaffolds.

C. Computational Analysis

The computational analysis was carried out in the *Ansys* program, and this was performed with the foot alone and with the fully assembled prosthesis. For both analyses, two cases were made: one with a 100kg load and the other with a maximum 200kg charge. The first step to do the static structural analysis of the mechanism was to export the assembly to the program and mesh it. The parameters of the mesh are seen in Table II. In the fully assembled prosthesis case, the external load was applied to the knee, but the force was set to be above the ankle for the foot analysis. Besides those mentioned above, the areas of contact with the ground were chosen as fixed points; that is, the part of the prosthesis at the level of the metatarsal bones and the lower part of the heel. This can be seen in Figure 6.

Table II
STATIC ANALYSIS PARAMETERS

Study case	Nodes	Elements	Connections
Foot	11076	1665	0
Fully assembled prosthesis	33823	12906	21

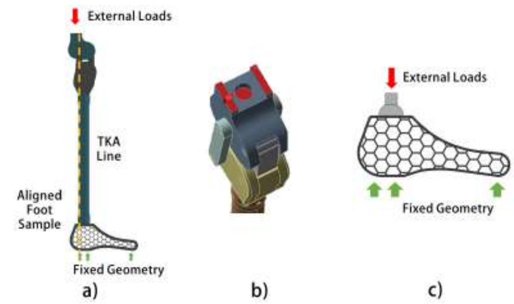

Figure 6. a) Direction of the load applied to the fully assembled prosthesis. b) Selected areas (red) in which the forces of 981N and 1962N were applied to the assembly. c) Direction of the load applied for the foot simulation.

V. RESULTS

A. Trajectory tracking

The comparison between the trajectories of points N and F with their respective reference is shown in Figure 7. An average relative error of points N and F of $Err_E = 0.059\%$ and $Err_F = 0.31\%$ respectively was obtained. With maximum error values of $Err_{max,N} = 0.20\%$ and $Err_{max,F} = 1.28\%$. The design parameters (with measurements in millimeters) obtained with the reference data are: $O = [-23.68, -70.32]$, $A = [-28.85, -26.58]$, $E = [-8.25, -26.58]$ and $U = [1.67, -79.10]$. Also, the ICR trajectory during full knee flexion presented values of $\gamma = 47.65$mm, and $\delta = 264.95$mm.

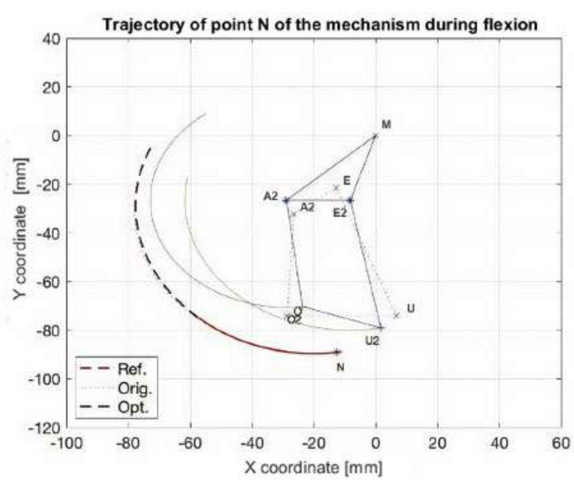

Figure 7. Comparison between the optimized trajectory of point N and the reference trajectory. It can be seen in blue solid lines the arrangement of the links after being optimized, with their respective reference (red lines).

The comparison between prosthesis flexion and knee angle during the gait cycle is shown in Figure 8. It is observed that a maximum error of 7.93% was obtained. Nonetheless, the trajectory tracking evaluation of the experimental model had a maximum error between the experimental and analytical model of 0.01mm.

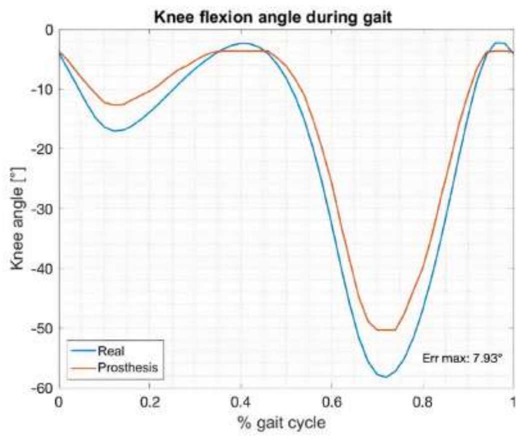

Figure 8. Knee flexion angle during gait. The reference data, denoted as a blue line, was obtained from a normal gait processed in the *OpenSim* software. The red line represents the propose model.

B. Shock absorb

The damping analysis was divided into two sections; during ground contact (0-40% of the gait cycle) and after detachment. The comparison between the reference moment and that obtained with the dampers. Values of the elastic constant k_i and the damping coefficient δ_{ki} corresponding to each section $(i = 1, 2)$ are: $k_1 = 2.268$, $\delta_{k1} = 0.001$, $k_2 = 0.0125$, $\delta_{k2} = 0.0203$.

C. Finite Element Analysis

In Figure 9, it can be seen that the maximum total deformation of the foot during compression is 0.01889. This means that the deformation that could be produced during the gait cycle is minimal. In the case of the equivalent stress, the maximum value was 17.088MPa. The same results were obtained in both cases, i.e. for the load of 100kg and 200kg.

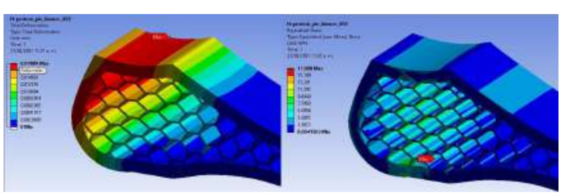

Figure 9. Foot simulation: Total deformation (Left) and Equivalent Von-Mises Stress (Right).

From the knee, pylon and foot simulations, it can be seen that the maximum total deformation was 0.58817. Meaning that the deformation in the area of most significant risk is within a safe area for the operability of the prosthesis. Also, the results with 100kg and 200kg were the same. This is the properties that the aluminum and carbon fibre have, which provide enough resistance to deformation and the flexibility necessary to cushion the stress at which the prosthesis is subjected. The scaffolding system was implemented to reduce weight and rigidity. The type of manufacturing with carbon fiber can include additive manufacturing in 3D or alternatively by injection of some alternative polymer such as polyurethane. On the other hand, the equivalent stresses on both loads applied, the maximum value can be observed in the anchorage between knee and pylon, notwithstanding this value remains lower than the aluminum tensile strength, despite maximum value, the majority design remains on the minimum of $454.19 \cdot 10^{-3}$. Thus the selection of the Al-7068 provides stability and hardness desired.

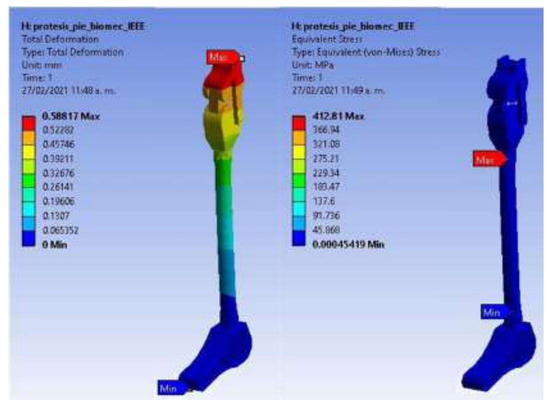

Figure 10. Lower limb prosthetic simulation: Total deformation (Left) and Equivalent Von-Mises Stress (Right).

VI. Discussion

The proposed methodology allows the design of customized modular limb prosthesis able to follow the trajectory of healthy walking by modelling in OpenSim the polycentric movement of the knee through the four-bar mechanism. As seen in Figure 2, points E and U are joined by twin bars at the sides of the mechanism, while a bar joins points O and A, this is located on the symmetry axis, which allows the addition of mechanical barriers to prevent hyper-extension and hyper-flexion. On the other hand, the optimizer can be modified to meet the specific needs of each patient. The material selection played an important role in knowing that the prosthesis would withstand the patient's total weight and two times this value. In the end, it was seen that the knee, pylon and foot would have a maximum total deformation of 0.58817, whereas the maximum stress was $454.19 \cdot 10^{-3}$MPa. This value was always above the tensile strength that the materials can withstand, meaning that the mechanism would not suffer any structural deformation. Furthermore, the hexagonal lattice geometry reduced the material by more than 70% of its original weight. And since carbon fiber was used for the foot, instead of a rigid material such as steel or aluminum, this allowed the foot to act as a damper with a maximum total deformation of 0.01889. The four-bar mechanism of the knee was capable of following the trajectory of the gait cycle with a maximum error of 7.93% during knee flexion. This was done by mimicking the polycentric motion of the human knee and assuming that the mechanism was an open kinematic chain.

VII. Conclusions

The first challenge for someone who suffers an amputation is having to adapt to a new lifestyle. Nonetheless, the prosthesis may become an important factor that helps the patient regain his autonomy. But, to do so, the prosthesis mechanism must follow the same trajectory that the leg has during the gait cycle. Simultaneously, the design process of a lower limb needs to be customized to meet each patient's specific needs and consider the amputation level and the socket's adaptation. However, the design of each socket should be personalized. The polycentric knee, pylon, and foot mechanism presented in this work can be replied to and adapted to any transfemoral prosthesis. Regarding the selection of materials, it was concluded that the mechanical and physical parameters allow determining if the load will be withstood, and the prosthesis will have a high index of functionality and durability. Finally, the generative design helped reduce the material to more than half its original weight, and it was seen that it did not compromise the resistance. Therefore, when manufacturing the foot with lattice optimization, the cost of the prosthesis will decrease. As part of the future work, it is worth mentioning the application of static, cyclic strength and cyclic resistance tests to the lower limb prostheses, following the ISO 10328:2016 norm requirements. Additionally, the norm ISO 16142-1:2016 must be followed for medical devices' essential safety and performance. This will be done at INCMNSZ. Furthermore, an extra evaluation for experimental corroboration of the trajectory would be performed using videogrametry with markers placed on points M, N and F of the prosthesis.

References

[1] N. Cisneros-González, I. de Jesús Ascencio-Montiel, V. N. Libreros-Bango, H. Rodríguez-Vázquez, Á. Campos-Hernández, J. Dávila-Torres, J. Kumate-Rodríguez, and V. H. Borja-Aburto, "Lower extremity amputation rates in diabetic patients," *Revista Médica del Instituto Mexicano del Seguro Social*, vol. 54, no. 4, pp. 472–479, 2016.

[2] C. L. McDonald, S. Westcott-McCoy, M. R. Weaver, J. Haagsma, and D. Kartin, "Global prevalence of traumatic non-fatal limb amputation," *Prosthetics and orthotics international*, 2020.

[3] C. E. Horne and J. A. Neil, "Quality of life in patients with prosthetic legs: a comparison study," *JPO: Journal of Prosthetics and Orthotics*, vol. 21, no. 3, pp. 154–159, 2009.

[4] M. Oosterhoff, J. H. Geertzen, and P. U. Dijkstra, "More than half of persons with lower limb amputation suffer from chronic back pain or residual limb pain: a systematic review with meta-analysis," *Disability and Rehabilitation*, pp. 1–21, 2020.

[5] L. J. Marks and J. W. Michael, "Clinical review-science, medicine, and the future: Artificial limbs," *BMJ-British Medical Journal-International Edition*, vol. 323, no. 7315, pp. 732–734, 2001.

[6] K. Edel, S. Hoac, and R. M. Shanabrook, "Developing a knee prosthesis," Ph.D. dissertation, Worcester Polytechnic Institute, 2021.

[7] J. F. Soriano, J. E. Rodríguez, and L. A. Valencia, "Performance comparison and design of an optimal polycentric knee mechanism," *Journal of the Brazilian Society of Mechanical Sciences and Engineering*, vol. 42, no. 5, pp. 1–13, 2020.

[8] P. Salas, M. Vergara, and S. Provenzano, "Prótesis de rodilla: Fundamentos teóricos y técnicas computacionales para su diseño knee prosthesis: theoretical foundations and computational techniques applied to its design," *Revista Ciencia e Ingeniería. Vol*, vol. 42, no. 1, 2021.

[9] A. Laclé and L. F. Valero-Juan, "Diabetes-related lower-extremity amputation incidence and risk factors: a prospective seven-year study in costa rica," *Revista Panamericana de Salud Pública*, vol. 32, pp. 192–198, 2012.

[10] M. W. Spong, S. Hutchinson, and M. Vidyasagar, *Robot modeling and control*. John Wiley & Sons, 2020.

[11] R. K. Mohanty, S. K. Sabut, and R. Mohanty, "Polycentric prosthetic knee joint: A review," 2017.

[12] S. L. Delp, F. C. Anderson, A. S. Arnold, P. Loan, A. Habib, C. T. John, E. Guendelman, and D. G. Thelen, "Opensim: Open-source software to create and analyze dynamic simulations of movement," *IEEE Transactions on Biomedical Engineering*, vol. 54, no. 11, p. 1940–1950, 2007.

[13] A. Seth, J. L. Hicks, T. K. Uchida, A. Habib, C. L. Dembia, J. J. Dunne, C. F. Ong, M. S. DeMers, A. Rajagopal, M. Millard *et al.*, "Opensim: Simulating musculoskeletal dynamics and neuromuscular control to study human and animal movement," *PLoS computational biology*, vol. 14, no. 7, p. e1006223, 2018.

[14] A. M. M. Nogueras, J. I. C. Arenillas, J. O. Rodríguez, F. B. Iglesias, and C. S. Sánchez, "Fases de la marcha humana," *Revista iberoamericana de fisioterapia y kinesiología*, vol. 2, no. 1, pp. 44–49, 1999.

[15] A. S. Arnold, M. Q. Liu, M. H. Schwartz, S. Ounpuu, and S. L. Delp, "The role of estimating muscle-tendon lengths and velocities of the hamstrings in the evaluation and treatment of crouch gait," *Gait & posture*, vol. 23, no. 3, pp. 273–281, 2006.

[16] S. L. Delp, F. C. Anderson, A. S. Arnold, P. Loan, A. Habib, C. T. John, E. Guendelman, and D. G. Thelen, "Opensim: open-source software to create and analyze dynamic simulations of movement," *IEEE transactions on biomedical engineering*, vol. 54, no. 11, pp. 1940–1950, 2007.

[17] S. L. Delp, J. P. Loan, M. G. Hoy, F. E. Zajac, E. L. Topp, and J. M. Rosen, "An interactive graphics-based model of the lower extremity to study orthopaedic surgical procedures," *IEEE Transactions on Biomedical engineering*, vol. 37, no. 8, pp. 757–767, 1990.

[18] M. L. Strydom, A. Banach, J. Roberts, R. Crawford, and A. T. Jaiprakash, "Kinematic model of the human leg using dh parameters," *IEEE Access*, vol. 8, 2020.

[19] R. L. Norton, "Four-bar and geared five-bar linkage analysis programs for the apple computer," *Mechanism and machine theory*, vol. 20, no. 4, pp. 313–320, 1985.

[20] G. Bovi, M. Rabuffetti, P. Mazzoleni, and M. Ferrarin, "A multiple-task gait analysis approach: kinematic, kinetic and emg reference data for healthy young and adult subjects," *Gait & posture*, vol. 33, no. 1, pp. 6–13, 2011.

[21] C. Quintero-Quiroz and V. Z. Pérez, "Materiales en interfaces y encajes ortoprotésicos de miembro inferior: Evolución y problemas dermatológicos asociados/materials for lower limb prosthetic and orthotic interfaces and sockets: Evolution and associated skin problems," *Revista de la Facultad de Medicina*, vol. 67, no. 1, p. 117, 2019.

[22] V. Faulkner, M. Field, J. W. Egan, and N. G. Gall, "Evaluation of high strength materials for prostheses," *Orthot Prosthet 40 (4), 44*, vol. 58, 1987.

[23] M. Frank, "Evaluation of mechanical properties in titanium (ti)-based pylon component upon friction stir processing," *J Biomed Eng*, vol. 1, pp. 1–8, 2016.

[24] M. Mori, K. F. MacDorman, and N. Kageki, "The uncanny valley [from the field]," *IEEE Robotics & Automation Magazine*, vol. 19, no. 2, pp. 98–100, 2012.

[25] C. Radcliffe, "Four-bar linkage prosthetic knee mechanisms: kinematics, alignment and prescription criteria," *Prosthetics and orthotics international*, vol. 18, no. 3, pp. 159–173, 1994.